HHS Public Access

Author manuscript

Dev Dyn. Author manuscript; available in PMC 2015 May 04.

Published in final edited form as:

Dev Dyn. 2014 April ; 243(4): 601–611. doi:10.1002/dvdy.24100.

Small Leucine Rich Proteoglycans Exhibit Unique Spatiotemporal Expression Profiles During Cardiac Valve Development

Loren E. Dupuis[1] and **Christine B. Kern**[1,*]

[1]Department of Regenerative Medicine and Cell Biology, Medical University of South Carolina, Charleston, SC 29425

Abstract

Background—Small Leucine Rich Proteoglycans (SLRPs) play a role in collagen fiber formation and also function as signaling molecules. Given the importance of collagen synthesis to the cardiovascular extracellular matrix (ECM), we examined the spatiotemporal expression of SLRPs, not previously investigated in the murine heart.

Results—Cardiac expression using antibodies specific for biglycan (BGN), decorin (DCN), fibromodulin (FMOD) and lumican (LUM) revealed distinct patterns among the SLRPs in mesenchymal-derived tissues. DCN showed the most intense localization within the developing valve cusps, while LUM was evident primarily in the hinge region of postnatal cardiac valves. BGN, DCN and FMOD were immunolocalized to regions where cardiac valves anchor into adjacent tissues. Medial (BGN), and adventitial (BGN, DCN, FMOD and LUM) layers of the pulmonary and aortic arteries also showed intense staining of SLRPs but this spatiotemporal expression varied with developmental age.

Conclusions—The unique expression patterns of SLRPs suggest they have adapted to specialized roles in the cardiovascular ECM. SLRP expression patterns overlap with areas where TGFβ signaling is critical to the developing heart. Therefore we speculate that SLRPs may not only be required to facilitate collagen fiber formation but may also regulate TGFβ signaling in the murine heart.

Keywords

Valves; Biglycan; Decorin; Fibromodulin; Lumican; Arterial wall

INTRODUCTION

How the mature extracellular matrix (ECM) is generated from mesenchymal-derived tissues is a poorly understood process yet profoundly affects the biomechanical properties of the cardiac structures and also influences cell behavior and phenotype. In early cardiac development the formation of the endocardial cushions, which give rise to the mature septal and valve structures of the adult heart, requires the large aggregating ECM proteoglycan

[*]denotes corresponding author: 171 Ashley Avenue, Basic Science Building 647, Charleston SC, 29425, kernc@musc.edu.

versican (Mjaatvedt et al., 1998). However, elongation of the endocardial cushions requires ECM remodeling of the provisional ECM concomitant with ECM versican cleavage (Dupuis et al., 2011; Dupuis et al., 2013). Fibrillar collagen formation occurs throughout cardiac valve maturation within the cusps as well as in the hinge and annulus (aortic root), regions that anchor valves. The requirement for appropriate collagen formation is supported by the fact that mutations in collagen genes lead to cardiac valve disease (Miller and Tyagi, 2002) and aortic aneurisms (COL3A1) (Kontusaari et al., 1990). In addition, several syndromes that result from mutations in collagen genes including Ehlers-Danlos syndrome (EDS), give rise to a variety of cardiovascular defects (Callewaert et al., 2008; Melis et al., 2012). Although the mature cardiovascular matrix is dependent on collagen fiber formation the role of non-collagen ECM components that facilitate their assembly have not been thoroughly studied.

The SLRPs (Small Leucine Rich Proteoglycans) are a family of ECM proteins that play a key role in the formation and/or assembly of collagen fibers in skeletal muscle (Tingbo et al., 2012) tendon and cornea (Chakravarti, 2002; Jepsen et al., 2002). There are four/five classes of SLRPs that contain an N-terminal variable domain rich in either sulfated tyrosines (Onnerfjord et al., 2004) or acidic amino acids and a second highly conserved domain of leucine-rich repeats (LRR) (Kalamajski and Oldberg, 2010). The collagen-binding motifs are located within the LRR repeats. Although the collagen-binding SLRPs are highly homologous, they are differentially expressed in normal tissues and during ECM remodeling. In addition SLRPs show differential collagen-binding affinities and play distinct roles in collagen assembly and matrix turnover suggesting the SLRPs have evolved to generate the highly specialized connective tissues required in complex vertebrates (reviewed (Kalamajski and Oldberg, 2010)). Most of the class I and class II SLRPs contain glycosaminoglycan (GAG) chains, with the exception of asporin, which plays a role in bone mineralization (Kalamajski et al., 2009). The type of glycosylations, chondroitin/dermatan/heparin sulfate as well as the identity and number of GAG chains influences collagen binding of SLRPs. The SLRPs are referred to as ‘small proteoglycans’ to distinguish them from the large aggregating proteoglycans versican and aggrecan. Gene-targeting mouse models of the four collagen-binding SLRPs have been generated (biglycan (BGN) (Furukawa et al., 2009), decorin (DCN) (Schonherr et al., 2004), fibromodulin (FMOD) (Goldberg et al., 2011) and lumican (LUM) (Jepsen et al., 2002)) and further document the critical role of these SLRPs in connective tissue and bone formation through collagen binding. Although mice deficient in SLRPs have also been referred to as *in vivo* models for Ehler-Danlos syndrome and other diseases related to collagen deficiencies (Ameye and Young, 2002), their spatiotemporal expression and role in murine cardiovascular tissues has not been previously described.

In addition to providing a structural role in matrix assembly, SLRPs have emerged as essential cell signaling components, which influence cell behaviors including proliferation, differentiation and migration. These functions are due to the ability of SLRPs to interact directly with cytokines and ligands as well as cell surface receptors. The ability of SLRPs to inhibit growth is due in part to their ability to bind TGFβ ligand (reviewed (Iozzo and Schaefer, 2010)). Recent reports from human patients and mouse models with cardiac valve

disease have revealed that fibrillin-1, a fibrous structural component of the ECM, plays a critical role in TGFβ activation during disease (Doyle et al., 2012). Collectively these studies suggest that a better understanding of components that comprise the specialized ECM architecture of the cardiovascular structures will likely reveal additional aspects of ECM-cell signaling that are critical for maintaining homeostasis in the adult and preventing disease.

In this study we evaluated the normal spatiotemporal cardiovascular expression of BGN and DCN as well as FMOD and LUM, collagen-binding, GAG containing class I, and II SLRPs respectively. Here we examine the differential expression patterns in the developing cardiovascular structures, focusing on the arterial walls and cardiac valves that reveal highly specific and specialized localization in maturing ECM. In addition we identified how the histological techniques affect sensitivity and non-specific staining of antibodies directed against these SLRPs in murine cardiovascular tissues. Finally, given the increasing number of viable mouse models with cardiovascular phenotypes, determining the normal expression profile of SLRPs may be a resource for the molecular characterization of ECM remodeling defects pertaining to both cardiovascular development and disease.

RESULTS

SLRPs are present in both the mesenchymal and myocardial structures in early (E10.5) cardiovascular development

The immunolocalization of BGN, DCN, FMOD and LUM in E10.5 murine hearts revealed FMOD and LUM exhibited significant staining localized to the myocardium (Fig. 1C′, C ″, D′, D″, solid arrows). In addition, LUM appeared in the non-cellularized regions of both the outflow tract (OFT) and atrioventricular (AVC) (Fig. 1D′, D″, open arrows) cushions whereas FMOD was virtually absent (Fig. 1C′, C″, open arrows). BGN showed slight punctate staining within undifferentiated myocardium (defined as actively proliferating and α-sarcomeric actin and α-smooth muscle actin positive) and was visible at high magnification (Fig. 1A′, A″, solid arrows). When compared to an IgG control (Fig. 1E–E″), DCN was not detected in the E10.5 heart but was visible in non-cardiovascular tissues (Fig. 1B, solid arrowhead). BGN appeared as insoluble splotches that essentially ‘floated away’ from the tissue. However, using a post-fixation technique, the staining adhered to the tissue and allowed more consistent localization within early cardiovascular tissues. Therefore all four SLRPs examined showed an immunolocalization pattern distinct from each other in the E10.5 murine heart. At this stage immunolocalization of BGN and DCN required the precipitating (acetic acid-alcohol based) Amsterdam (Amst) fixative, while FMOD and LUM utilized the cross-linking fixative paraformaldehyde (para).

Biglycan, decorin, fibromodulin and lumican were immunolocalized adjacent to elongating cardiac valves and within the developing arterial walls at embryonic day 14.5

At E14.5 DCN immunostaining (Fig. 2G–L) was the most prominent of all SLRPs and localized within all cusp commissures, the area where the valve mesenchyme and myocardium meet and where the valve hinge forms and anchors into surrounding myocardial or arterial tissue (Fig. 2G, I, J, open arrows). The arterial walls of the pulmonary artery and aorta (PA and Ao respectively) expressed BGN, DCN, FMOD and LUM (Fig.

2A, B, D, E, G, H, J, K, M, N, S, T, open arrowheads) however the staining pattern of BGN differed from the other SLRPs. DCN, FMOD and LUM were localized to the adventitial layer while BGN was more widely distributed throughout the medial layer and coincident with early elastin localization (Fig. 2B, D, E, open arrowheads). At this stage FMOD and LUM required para fixative for detection in the arterial walls as evidenced by the lack of staining in Amst fixative (Fig. 2Q, W). BGN, FMOD, and LUM were detected in the myocardium adjacent to the valve mesenchyme (Fig. 2C, O, P, U, V, solid arrows); this myocardium is referred to as 'transient myocardium' since it disappears during development through an unknown process. In the developing mitral valve (MV) leaflets, LUM was the only SLRP examined that showed significant staining above background, and also required para fixation (Fig. 2X, solid arrowhead).

Biglycan, decorin, fibromodulin and lumican were localized within the valves, annulus, arterial walls and epicardium at postnatal day 0 suggesting SLRPs play a role in generating specialized collagen-rich matrix

At postnatal day 0 (P0) BGN (Fig. 3A–B), FMOD (Fig. 3K–L) and LUM (Fig. 3P–P′) exhibited intense immunolocalization in the sites where PV cusps attach to the arterial wall. DCN was more prominent than the other SLRPs throughout the cusps of the PV, AV, MV (Fig. 3F–I, solid arrowheads) and TV (not shown). For all SLRPs analyzed, use of the Amst fixative for the postnatal valves allowed more readily detectable immunolocalization with a concomitant reduction of background fluorescence compared to the para fixed hearts at P0 (Fig. 3A–B, F–G, K–L, P–Q). BGN, DCN and FMOD were localized at the myocardial attachment regions of the AV cusps (Fig. 3C, H, M, solid arrows) while antibodies against LUM revealed significantly weaker immunostaining at this juncture (Fig. 3R, solid arrows). The Ao showed intense immunostaining with DCN and LUM antibodies in the adventitial layer (Fig. 3H, R, open arrowheads) while BGN was localized within the medial layer of the arterial wall (Fig. 3C, open arrowhead). At P0, FMOD was absent from the arterial walls of the PA and Ao (Fig. 3M). In the MV, BGN, DCN, and FMOD showed high expression in areas where the leaflets anchor into the myocardium (Fig. 3D, I, N, solid arrows) while LUM was absent from these regions. DCN and LUM immunolocalization revealed intense staining in the epicardium, however DCN was localized to the ECM space while LUM was found subjacent to the epicardial epithelial cell layer (Fig. 3J, T, open arrows). BGN was also present in the epicardium but at lower levels (Fig. 3E, open arrows).

Maturation of the semilunar valve cusps and annulus correlated with intense immunolocalization and unique expression patterns of collagen-binding SLRPs

At 1 month (1mo) regions where the PV and AV cusp hinges anchor to surrounding tissues stain intensely with antibodies against BGN, DCN and FMOD (Fig. 4A–B′, E–F′, I–J′, solid arrows), but were void of LUM in the AV (Fig. 4N, N′) and LUM was just above background levels in the PV (Fig. 4M, solid arrow). With the exception of DCN, the collagen-binding SLRPs were not detected in the 1 mo PV cusps (Fig. 4A, E, I, M). In the AV cusp hinge, BGN, DCN, FMOD and LUM were present (Fig. 4B, B′, F, F′, G, J, J′, N, N′, solid arrowhead). BGN, DCN, and LUM showed expression in the Ao, but FMOD was not detected (Fig. 4B″, F″, J″, N″, open arrowheads). The Ao showed intense immunostaining of BGN and DCN in the adventitial layer (Fig. 4B″, F″, open arrowheads). BGN was also

expressed throughout the medial layer of the wall whereas LUM staining was present in the outer aspect of the medial layer (Fig. 4B″, N″, open arrowhead). In the distal cusps of the AV, fixed with para, immunolocalization revealed staining of BGN, DCN and LUM (Fig. 4C, G, O, solid arrowhead), with DCN more readily detected than the other SLRPs examined. In the MV, BGN, DCN, FMOD and LUM were all detected throughout the leaflets (Fig. 4D, H, L, P, solid arrowheads). The specific MV immunolocalization of SLRPs differed; for example, BGN and LUM staining was concentrated in the tip of the anterior leaflet (AL) while DCN staining was observed throughout. The fibrous attachment of the MV posterior leaflet (PL) showed strong staining of BGN, DCN and FMOD (Fig. 4D, H, L, solid arrows) but LUM was virtually absent (Fig. 4P). At 1 mo the chordae tendineae are developing near the anchoring junction of the leaflets to the papillary muscles; expression of BGN, DCN, FMOD and LUM all extended up into the forming tendinous chords (Fig. 4D, H, L, P solid arrows).

Mature connective tissue in the murine heart exhibited high levels of SLRPs in the cardiac valves, as well as the arterial walls of the pulmonary and aortic arteries

Generally, in the adult murine cardiovascular ECM, immunodetection of BGN, DCN, FMOD and LUM revealed stronger staining than developmental stages (Fig. 5). In the semilunar valves BGN (Fig. 5A–B′, solid arrowheads), DCN (Fig. 5D–E′, solid arrowheads) and LUM (Fig. 5J–K′, solid arrowheads) were present throughout the cusps while FMOD was absent (Fig. 5G–H′). Within the PA and Ao, BCN, DCN, and LUM exhibited strong immunostaining; however, FMOD was restricted to regions where the aortic hinge anchored into the surrounding arterial tissue (commissures) and was void in regions of the arterial walls that were not associated with cusps (Fig. 5B, E, H, K, open arrowheads). BGN, DCN, and LUM were also expressed at dissimilar levels and in different layers of the arterial walls. Immunolocalization of DCN and LUM revealed high levels in the adventitia (Fig. 5D, E, J, K, open arrowheads) whereas BGN was expressed throughout the medial layer with stronger staining than earlier time points (Fig. 5A, B, open arrowheads). The MV expressed high levels of BGN, DCN, FMOD and LUM (Fig. 5C′, F′, I′, L′, open arrows) with similar intensity and localization. DCN exhibited the most restricted expression within the atrial layer (Fig. 5F′, open arrows). Images presented in Fig. 5 were from Amst fixed tissue however patterns of expression were identical in para as well as cryo preserved sections. Generally para fixation exhibited higher levels of background while cryosections distorted morphology thus reducing accuracy in identifying discrete differences in the SLRP staining patterns (data not shown).

Schematic summary reveals complex and differential expression patterns of BGN, DCN, FMOD and LUM in the ascending arterial walls and cardiac valves

The schematic of the PV and PA (Fig. 6A) at different stages indicates BGN (purple, E14.5) immunolocalized to the medial layer of the PA; this pattern was maintained throughout development and within the adult heart. BGN was also evident in the PV cusps at P0 and in the adult where coaptation occurs. Importantly the region of coaptation in PV cusps undergoes the most notable structural changes from 1 mo where BGN was absent. BGN was also found in regions where the PV cusps anchor (squares and rectangles) however its expression patterns were diverse and transient when compared between stages.

Immunolocalization of DCN (green) revealed PA staining in the outer layers at E14 and from P0 forward DCN IHC exhibited intense staining within the adventitia. The regions where the AC and RC mesenchyme is adjacent to the myocardium (open arrow) also showed DCN immunolocalization at E14.5. However, by P0 DCN expression was increased and localized throughout the PV cusps. Similar to BGN, DCN was concentrated within the annulus surrounded by the AC only (*). The intensity of DCN IHC in the PV cusps was significantly less at 1 mo compared to P0 and adult stages. FMOD (red) showed the most restricted and concentrated expression of all SLRPs examined. At E14.5 FMOD was localized within the myocardium adjacent to the AC and RC (solid arrow). As the hinge of the PV cusps narrowed during valve maturation, FMOD expression increased with foci of intense IHC staining where cusps anchor to the arterial wall and within the annulus at P0 and 1 mo. In the adult heart FMOD was deposited in the PA and in discrete foci above the RC attachment and within the AC annulus, but its overall expression was reduced compared to earlier stages. FMOD appeared in the PV cusps transiently after birth but was not present at later stages. Similar to FMOD, LUM (blue) was localized within the myocardium surrounding the valve mesenchyme of the AC and RC at E14.5 (solid arrows). During development LUM expression increased and by P0 was evident throughout the PV cusps and concentrated where cusps anchor into the PA. LUM deposition was also noted in the epicardium at P0 and in the adult. While LUM expression was not found in 1 mo PV cusps, there were significant levels of LUM in adult PV cusps.

The expression patterns of the SLRPS in the developing AV and Ao is summarized in Figure 6B and resembles expression of the PV and PA, respectively. For example at E14.5 DCN was localized within the valve mesenchyme that borders the myocardium (open arrow), while FMOD and LUM were present within the adjacent myocardial tissue (solid arrows). In general, the expression of the SLRPs within the AV cusps was higher than in the PV cusps. The annulus regions where the RCC and LCC anchor (rectangles) showed intense expression of BGN, DCN, and FMOD from birth; however intense LUM staining was found almost exclusively in the mature ECM of the adult AV annulus. The predominant SLRP expression in the adult AV annulus at the juncture where cusps anchor was distinctly different from the PV annulus where SLRP expression was reduced in the adult compared to 1 mo and P0. However the arterial wall expression of SLRPs in the aorta was similar to the PA with BGN localized within the medial portion of the maturing vessel wall in contrast to DCN and LUM found predominantly in the outer layers and mature adventitia.

The schematic diagram in Figure 6C shows SLRP expression in the MV. The overall IHC patterns of BGN, DCN, FMOD and LUM were significantly different from each other both with respect to spatiotemporal localization and intensity. In contrast to semilunar valves LUM was noted in MV leaflets at E14.5 however both its pattern and IHC intensity increased during MV maturation similar to the PV and AV cusps. BGN IHC showed intense staining in regions where the (anterior leaflet) AL anchors into the myocardium at P0 (solid arrow) and the expression of BGN increased during MV maturation. DCN was observed throughout the PL from P0 through adult. Unlike the semilunar valves, FMOD was present in the adult MV leaflets. The base of the leaflets (open arrowheads) and the tip (closed arrowheads) showed differential patterns of SLRP expression. Overall the adult MV leaflets showed the most prominent SLRP expression compared to other stages, a trend that was

similar to the adult semilunar valve cusps. However, the mature ECM where leaflets anchor into the myocardium showed an overall reduction in SLRP expression compared to 1 mo and P0, a staining pattern more similar to the ECM that anchors the PV than the AV.

DISCUSSION

The individualized expression pattern of BGN, DCN, FMOD and LUM accentuates the specialized ECM regions throughout the developing and mature murine heart, and serves to further delineate differences in the cardiovascular ECM architecture. Notably to achieve reproducible IHC the type of fixation, post-fixation and antigen unmasking techniques were different among the SLRP antibodies and even differed among developmental stages. Therefore the interpretation of our results is based on multiple fixations and samples in an effort to obtain the most sensitive IHC readouts, where background was minimal and a low threshold of specific immunofluorescence was observed. The most prominent expression of the SLRPs was found in postnatal cardiac valves and their supportive structures (Fig. 6). The spatiotemporal pattern of SLRP expression also unveils a role for SLRPs in developmental transitions from a provisional ECM rich in the aggregating proteoglycan versican to an organized ECM containing collagen and elastin. The high levels of SLRP expression in the tissues that anchor the valve cusps suggests their involvement in generating the mature ECM required for strength and flexibility in the adult mouse heart. Given the ability of SLRPs to bind growth factor ligands and receptors, the complex and unique cardiac expression may also reveal intracellular signaling and phenotypes of cells enmeshed within specialized cardiovascular ECM. In addition, identification of core proteoglycans within the developing cardiovascular ECM may also facilitate molecular characterization of developmental cardiovascular anomalies in gene-targeted mouse models.

The high levels of BGN, DCN, FMOD and LUM expression in postnatal cardiac valves is consistent with a major role of the SLRPs in the assembly of specialized collagen matrices in response to increases in mechanical load (Kalamajski and Oldberg, 2010). Similar to the expression of SLRPs in tendons, BGN, FMOD and LUM were highly expressed in tissue foci that connect the cardiac valve cusps to the arterial wall and ventricular myocardium. Gene-targeted mouse models demonstrate that BGN and LUM are involved in crosslinking the initial collagen fibrils in skin and developing tendon while DCN and FMOD are required for generating thick collagen fibrils (reviewed (Kalamajski and Oldberg, 2010)). The tendon fibrils in decorin deficient mice have a broader range of diameter suggesting that decorin restrains the collagen fibrils to generate a more uniform and thinner diameter (Danielson et al., 1997; Seidler et al., 2005; Iwasaki et al., 2008). In contrast fibromodulin deficient tendons contain thinner collagen fibrils suggesting that it plays a role in connecting rather than constricting collagen fibril growth (Ezura et al., 2000). However, in the developing murine heart, DCN and FMOD were found at early stages of collagen assembly. DCN levels remained high in the adult valve cusps while FMOD was virtually absent in the adult valves but present in adjacent tissues that anchor the semilunar valve cusps. Therefore the expression of DCN and FMOD in cardiac valves may indicate a involvement in the initial collagen fiber formation, as well as generation of larger collagen fibers required in the adult cardiac valves and their supportive structures. Alternately, the abundant adult valve expression of DCN may indicate the requirement for continual collagen fiber formation due

to biomechanical breakdown. Notably we also observed differences in the SLRP expression between the PV and AV. This is similar to results from a proteomic approach where BGN was enriched in the AV compared to the PV and consistent with differences in biomechanical forces between the valves (Angel et al., 2011). In porcine valves collagen-binding proteoglycans also increase after birth concomitant with increases in mechanical load and vascular resistance (Stephens et al., 2010). Biglycan localization in human valves coincides not only with regions that stain for collagen but also for elastin (Gupta et al., 2009) a finding consistent with our results. Although each of the SLRPs examined exhibited a unique pattern of expression within the heart, there were regions of overlapping immunolocalization in all areas of the cardiovascular ECM. Therefore investigation using mouse models deficient in one versus multiple SLRPs may give insight into potential functional redundancy or, determine if mammalian SLRPs provide uniquely specialized roles in collagen assembly and maintenance throughout the murine heart.

Aside from their structural role the ability of SLRPs to bind and to sequester growth factors implicates their involvement in the regulation of cell behavior and phenotype (reviewed (Iozzo and Schaefer, 2010)). Both BGN and DCN bind TGFβ ligand, and are expressed in the cardiac valves and ascending aortic artery, where TGFβ signaling also plays a critical role (Doyle et al., 2012). The antiproliferative role of decorin is also well documented (Yamaguchi and Ruoslahti, 1988; Yamaguchi et al., 1990; Hildebrand et al., 1994) due to its ability to effect TGFβ signaling (Yamaguchi et al., 1990) a property also shared by BGN and FMOD (Hildebrand et al., 1994). It has recently been shown that pSmad2, a mediator of TGFβ signaling, may be critical for the onset of ECM transitions in the cardiac valve hinge (Dupuis et al., 2013); therefore SLRP expression during hinge formation may serve to down regulate TGFβ signaling by sequestering the TGFβ ligand(s) as prevalvular cells differentiate. In fact reports show BGN deficiency promotes myofibroblast formation and proliferation *in vitro* and *in vivo* (Melchior-Becker et al., 2011). Although ECM maturation often mirrors cell differentiation, the interconnection between ECM architecture and cell signaling programs within the developing heart remains poorly understood. The involvement of SLRPs in TGFβ signaling represents only one of many potential intersections of SLRPs in the regulation of cell signaling during cardiovascular development.

The expression of SLRPs in normal cardiac valves together with their role in collagen fiber assembly suggests that dysregulation of SLRPs may lead to cardiac valve disease. In aortic calcific disease previous studies have shown destruction of the normal matrix results in a dramatic reduction of DCN and FMOD (Matsumoto et al., 2012). Calcific nodules are devoid of DCN and BGN although these SLRPs remain adjacent to the nodule and within precalcific nodules (Stephens et al., 2011). Since DCN competes with asporin for binding sites on collagen, a reduction in DCN with a concomitant increase in asporin could promote mineralization and may contribute to calcific aortic valve disease progression. Recent reports also demonstrate that soluble BGN contributes to the pro-osteogenic effect of oxLDL in human aortic valve interstitial cells (Song et al., 2012). Pathogenesis of the myxomatous mitral valve also disrupts normal SLRP distribution (Gupta et al., 2009). Therefore changes in SLRP expression during the progression of cardiac valve disease is complex but given their involvement in both tissue integrity and cell signaling

understanding the role of these proteoglycans may give insight to both the etiology and progression of cardiac valve disease.

This study demonstrates the dynamic and complex expression patterns of the collagen-binding and GAG containing, SLRPs during cardiovascular development. SLRP expression also highlighted the intricate ECM architecture found within the developing and adult murine heart. These developmental SLRP expression data may provide a foundation that will advance our understanding of the interconnection between the biomechanical properties of cardiac tissues, cell phenotype and signaling when applied to mouse models with anomalies of cardiac disease. Given the dual role of SLRPs in tissue integrity and cell signaling, SLRPs also show promise as novel therapeutic targets and/or biomarkers for cardiovascular disease.

EXPERIMENTAL PROCEDURES

Mice

All mouse experiments were done under protocols approved by the Medical University of South Carolina IACUC. Mice used in this study were bred into C57BL/6.

Histology and Immunohistochemistry

Standard histological procedures were used (Kern et al., 2007). Biglycan antibody (LF-159) and fibromodulin antibody (LF150) were generous gifts from Dr. L. Fisher at the National Institute of Health. The lumican antibody was a gift from Dr. A. Oldberg, Lund University. Decorin antibody (AF1060) was purchased from R & D Systems Inc. Antibodies to α-sarcormeric actin (Sigma, A2172), and α-smooth muscle actin (Sigma, A 5228) were also utilized in this study to identify myocardial and smooth muscle cells respectively. Fluor-conjugated secondary antibodies were purchased from Jackson ImmunoResearch (West Grove, PA). Antibodies were used in murine tissues fixed in Amsterdam (Amst=35% methanol=35% acetone=5% acetic acid) (Dupuis et al., 2011) and 4% paraformaldehyde (para) as well as cryopreserved sections. All para fixed tissue was paired with citric acid antigen unmasking (H-3300, Vector laboratories, Burlingame CA). Imaging was performed on the Leica TCS SP5 AOBS Confocal Microscope System (Leica Microsystems Inc., Exton, PA). Post-fixation involved 80% ethanol for 5 minutes, followed by 50% ethanol for 5 minutes and then two rinses in phosphate buffered saline.

Acknowledgments

Grant Support:

American Heart Association: 10SDG2610168

National Institutes of Health: NIH RR 0164 34

The authors thank Matthew Berger, Vennece Fowlkes, Ariel Washington, Olivia Coco and Aimee Phelps for their histology expertise.

References

Ameye L, Young MF. Mice deficient in small leucine-rich proteoglycans: novel in vivo models for osteoporosis, osteoarthritis, Ehlers-Danlos syndrome, muscular dystrophy, and corneal diseases. Glycobiology. 2002; 12:107R–116R.

Angel PM, Nusinow D, Brown CB, Violette K, Barnett JV, Zhang B, Baldwin HS, Caprioli RM. Networked-based characterization of extracellular matrix proteins from adult mouse pulmonary and aortic valves. J Proteome Res. 2011; 10:812–823. [PubMed: 21133377]

Callewaert B, Malfait F, Loeys B, De Paepe A. Ehlers-Danlos syndromes and Marfan syndrome. Best Pract Res Clin Rheumatol. 2008; 22:165–189. [PubMed: 18328988]

Chakravarti S. Functions of lumican and fibromodulin: lessons from knockout mice. Glycoconj J. 2002; 19:287–293. [PubMed: 12975607]

Danielson KG, Baribault H, Holmes DF, Graham H, Kadler KE, Iozzo RV. Targeted disruption of decorin leads to abnormal collagen fibril morphology and skin fragility. J Cell Biol. 1997; 136:729–743. [PubMed: 9024701]

Doyle JJ, Gerber EE, Dietz HC. Matrix-dependent perturbation of TGFbeta signaling and disease. FEBS Lett. 2012; 586:2003–2015. [PubMed: 22641039]

Dupuis LE, McCulloch DR, McGarity JD, Bahan A, Wessels A, Weber D, Diminich AM, Nelson CM, Apte SS, Kern CB. Altered versican cleavage in ADAMTS5 deficient mice; a novel etiology of myxomatous valve disease. Dev Biol. 2011; 357:152–164. [PubMed: 21749862]

Dupuis LE, Osinska H, Weinstein MB, Hinton RB, Kern CB. Insufficient versican cleavage and Smad2 phosphorylation results in bicuspid aortic and pulmonary valves. J Mol Cell Cardiol. 2013; 60:50–59. [PubMed: 23531444]

Ezura Y, Chakravarti S, Oldberg A, Chervoneva I, Birk DE. Differential expression of lumican and fibromodulin regulate collagen fibrillogenesis in developing mouse tendons. J Cell Biol. 2000; 151:779–788. [PubMed: 11076963]

Furukawa T, Ito K, Nuka S, Hashimoto J, Takei H, Takahara M, Ogino T, Young MF, Shinomura T. Absence of biglycan accelerates the degenerative process in mouse intervertebral disc. Spine (Phila Pa 1976). 2009; 34:E911–917. [PubMed: 19940720]

Goldberg M, Marchadier A, Vidal C, Harichane Y, Kamoun-Goldrat A, Kellermann O, Kilts T, Young M. Differential effects of fibromodulin deficiency on mouse mandibular bones and teeth: a micro-CT time course study. Cells Tissues Organs. 2011; 194:205–210. [PubMed: 21597266]

Gupta V, Barzilla JE, Mendez JS, Stephens EH, Lee EL, Collard CD, Laucirica R, Weigel PH, Grande-Allen KJ. Abundance and location of proteoglycans and hyaluronan within normal and myxomatous mitral valves. Cardiovasc Pathol. 2009; 18:191–197. [PubMed: 18621549]

Hildebrand A, Romaris M, Rasmussen LM, Heinegard D, Twardzik DR, Border WA, Ruoslahti E. Interaction of the small interstitial proteoglycans biglycan, decorin and fibromodulin with transforming growth factor beta. Biochem J. 1994; 302 (Pt 2):527–534. [PubMed: 8093006]

Iozzo RV, Schaefer L. Proteoglycans in health and disease: novel regulatory signaling mechanisms evoked by the small leucine-rich proteoglycans. FEBS J. 2010; 277:3864–3875. [PubMed: 20840584]

Iwasaki S, Hosaka Y, Iwasaki T, Yamamoto K, Nagayasu A, Ueda H, Kokai Y, Takehana K. The modulation of collagen fibril assembly and its structure by decorin: an electron microscopic study. Arch Histol Cytol. 2008; 71:37–44. [PubMed: 18622092]

Jepsen KJ, Wu F, Peragallo JH, Paul J, Roberts L, Ezura Y, Oldberg A, Birk DE, Chakravarti S. A syndrome of joint laxity and impaired tendon integrity in lumican- and fibromodulin-deficient mice. J Biol Chem. 2002; 277:35532–35540. [PubMed: 12089156]

Kalamajski S, Aspberg A, Lindblom K, Heinegard D, Oldberg A. Asporin competes with decorin for collagen binding, binds calcium and promotes osteoblast collagen mineralization. Biochem J. 2009; 423:53–59. [PubMed: 19589127]

Kalamajski S, Oldberg A. The role of small leucine-rich proteoglycans in collagen fibrillogenesis. Matrix Biol. 2010; 29:248–253. [PubMed: 20080181]

Kern CB, Norris RA, Thompson RP, Argraves WS, Fairey SE, Reyes L, Hoffman S, Markwald RR, Mjaatvedt CH. Versican proteolysis mediates myocardial regression during outflow tract development. Dev Dyn. 2007; 236:671–683. [PubMed: 17226818]

Kontusaari S, Tromp G, Kuivaniemi H, Romanic AM, Prockop DJ. A mutation in the gene for type III procollagen (COL3A1) in a family with aortic aneurysms. J Clin Invest. 1990; 86:1465–1473. [PubMed: 2243125]

Matsumoto K, Satoh K, Maniwa T, Araki A, Maruyama R, Oda T. Noticeable decreased expression of tenascin-X in calcific aortic valves. Connect Tissue Res. 2012; 53:460–468. [PubMed: 22827484]

Melchior-Becker A, Dai G, Ding Z, Schafer L, Schrader J, Young MF, Fischer JW. Deficiency of biglycan causes cardiac fibroblasts to differentiate into a myofibroblast phenotype. J Biol Chem. 2011; 286:17365–17375. [PubMed: 21454527]

Melis D, Cappuccio G, Ginocchio VM, Minopoli G, Valli M, Corradi M, Andria G. Cardiac valve disease: an unreported feature in Ehlers Danlos syndrome arthrocalasia type? Ital J Pediatr. 2012; 38:65. [PubMed: 23158907]

Miller AD, Tyagi SC. Mutation in collagen gene induces cardiomyopathy in transgenic mice. J Cell Biochem. 2002; 85:259–267. [PubMed: 11948682]

Mjaatvedt CH, Yamamura H, Capehart AA, Turner D, Markwald RR. The Cspg2 gene, disrupted in the hdf mutant, is required for right cardiac chamber and endocardial cushion formation. Dev Biol. 1998; 202:56–66. [PubMed: 9758703]

Onnerfjord P, Heathfield TF, Heinegard D. Identification of tyrosine sulfation in extracellular leucine-rich repeat proteins using mass spectrometry. J Biol Chem. 2004; 279:26–33. [PubMed: 14551184]

Schonherr E, Sunderkotter C, Schaefer L, Thanos S, Grassel S, Oldberg A, Iozzo RV, Young MF, Kresse H. Decorin deficiency leads to impaired angiogenesis in injured mouse cornea. J Vasc Res. 2004; 41:499–508. [PubMed: 15528932]

Seidler DG, Schaefer L, Robenek H, Iozzo RV, Kresse H, Schonherr E. A physiologic three-dimensional cell culture system to investigate the role of decorin in matrix organisation and cell survival. Biochem Biophys Res Commun. 2005; 332:1162–1170. [PubMed: 15949467]

Song R, Zeng Q, Ao L, Yu JA, Cleveland JC, Zhao KS, Fullerton DA, Meng X. Biglycan induces the expression of osteogenic factors in human aortic valve interstitial cells via Toll-like receptor-2. Arterioscler Thromb Vasc Biol. 2012; 32:2711–2720. [PubMed: 22982459]

Stephens EH, Post AD, Laucirica DR, Grande-Allen KJ. Perinatal changes in mitral and aortic valve structure and composition. Pediatr Dev Pathol. 2010; 13:447–458. [PubMed: 20536360]

Stephens EH, Saltarrelli JG, Baggett LS, Nandi I, Kuo JJ, Davis AR, Olmsted-Davis EA, Reardon MJ, Morrisett JD, Grande-Allen KJ. Differential proteoglycan and hyaluronan distribution in calcified aortic valves. Cardiovasc Pathol. 2011; 20:334–342. [PubMed: 21185747]

Tingbo MG, Pedersen ME, Kolset SO, Enersen G, Hannesson KO. Lumican is a major small leucine-rich proteoglycan (SLRP) in Atlantic cod (Gadus morhua L.) skeletal muscle. Glycoconj J. 2012; 29:13–23. [PubMed: 22124673]

Yamaguchi Y, Mann DM, Ruoslahti E. Negative regulation of transforming growth factor-beta by the proteoglycan decorin. Nature. 1990; 346:281–284. [PubMed: 2374594]

Yamaguchi Y, Ruoslahti E. Expression of human proteoglycan in Chinese hamster ovary cells inhibits cell proliferation. Nature. 1988; 336:244–246. [PubMed: 3194009]

Bullet Points

Decorin is prominently expressed in maturing and adult cardiac valve cusps.

Biglycan expression is localized to regions of elastin synthesis in the arterial wall and cardiac valves.

Fibromodulin shows restricted expression in the annulus and valve hinge of the murine heart.

Lumican expression increases throughout postnatal cardiac valve maturation.

SLRP expression overlaps with regions of TGFβ signaling in the murine heart.

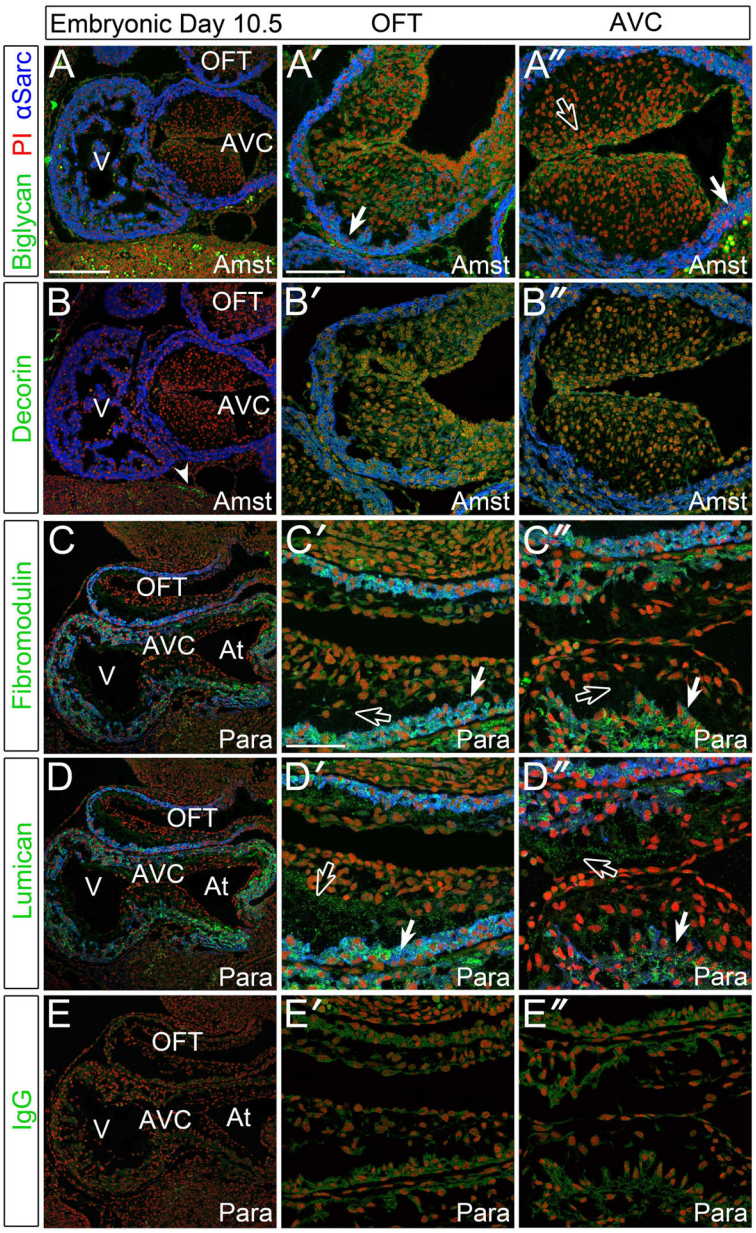

Figure 1. Biglycan, fibromodulin, and lumican were detected in the myocardium and endocardial cushions of E10.5 murine embryonic hearts

A–A″: Immunolocalization of biglycan (green) in Amsterdam (Amst) fixed tissue. **B–B″:** Decorin (green) immunolocalization in Amst fixed tissue. **C–C″**: Fibromodulin (green) staining in paraformaldehyde (Para) fixed tissue. **D–D″:** Immunolocalization of lumican (green) in Para fixative. **E–E″:** IgG (green) controls in sister sections. Solid arrows- myocardial staining; open arrows- endocardial cushion staining; arrowhead- non-cardiac DCN immunoreactivity. V- ventricle; AVC- atrioventricular cushions; OFT- outflow tract; At- atrium. Blue- alpha sarcomeric actin; red- propidium iodide. Scale bars: A= 200um, applies to B, C, D, E; A′= 100um, applies to A″, B′, B″; C′= 50um, applies to C″, D′, D″, E′, E″.

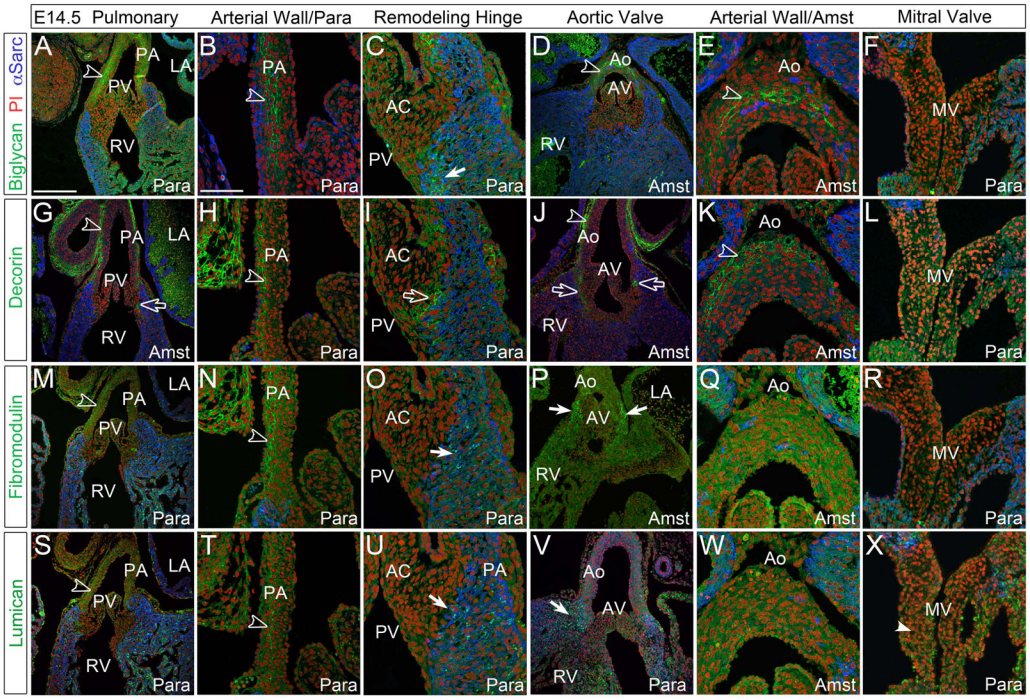

Figure 2. Small Leucine Rich Proteoglycans (SLRPs) were immunolocalized within arterial walls and associated with remodeling valve cusps/leaflets at E14.5

A–F: Biglycan (green), **G–L:** decorin (green), **M–R:** fibromodulin (green), and **S–X:** lumican (green) staining at E14.5. Open arrowheads- denote signal in the arterial wall; open arrow-juncture of valve mesenchyme and myocardium; solid arrows-immunoreactivity in the myocardium adjacent to prevalvular mesenchyme; solid arrowhead-staining in leaflet. LA- left atrium; RV- right ventricle; PA-pulmonary artery wall; PV-pulmonary valve; AC-anterior cusp of the PV; Ao-aortic wall; AV-aortic valve; MV-mitral valve; Para-paraformaldehyde fixed tissue; Amst- Amsterdam fixed tissue. Blue- alpha sarcomeric actin; red- propidium iodide. Scale bars: A= 200um, applies to D, G, J, M, P, S, V; B= 50um, applies to C, E, F, H, I, K, L, N, O, Q, R, T, U, W, X.

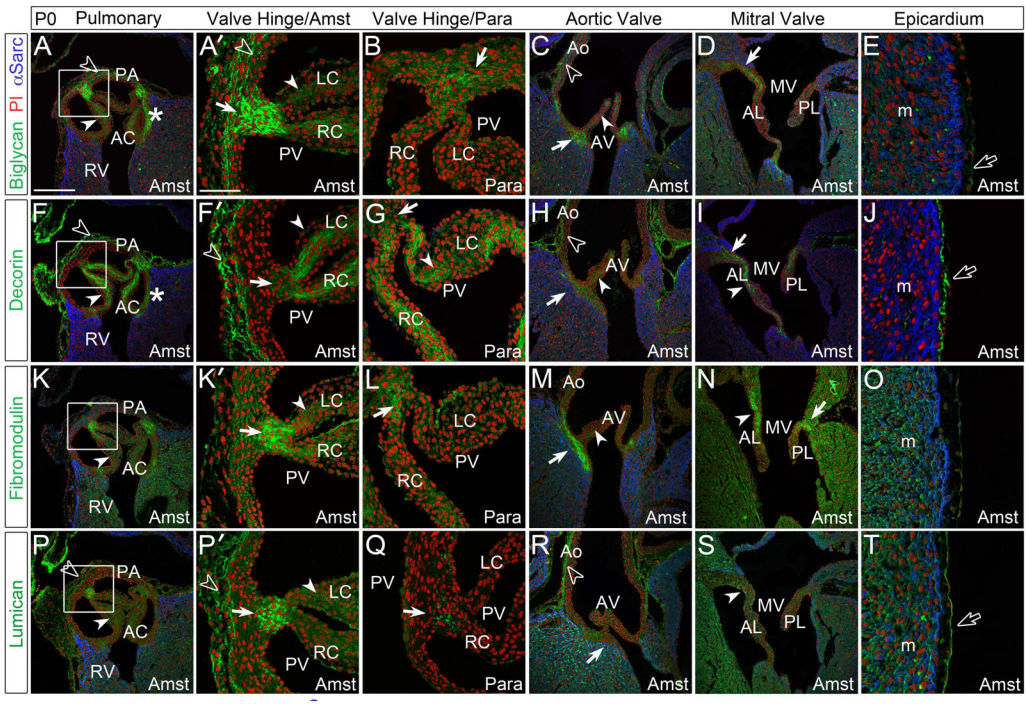

Figure 3. At postnatal day 0, Small Leucine Rich Proteoglycans (SLRPs) display differential staining patterns in the endocardial cushion derived structures of the maturing heart

A–E: Biglycan (green), **F–J:** decorin (green) **K–O:** fibromodulin (green) and **P–T:** lumican (green) immunolocalization in the pulmonary valve (PV), aortic valve (AV), mitral valve (MV) and epicardium. Boxes in A, F, K and P magnified in adjacent panel and designated with a prime. *-annulus region associated with the anterior cusp (AC) of the PV; solid arrows-regions where valve cusps or leaflets anchor into adjacent tissue; solid arrowheads-staining within the cusps or leaflets; open arrowheads- arterial wall staining; open arrows-epicardial staining. PA- pulmonary artery wall; RV-right ventricle; LC-left cusp of the PV; RC-right cusp of the PV; Ao-aortic wall; AL-anterior leaflet of the MV; PL-posterior leaflet of the MV. m- myocardium; Para- paraformaldehyde fixed tissue; Amst- amsterdam fixed tissue. Blue- alpha sarcomeric actin; red- propidium iodide. Scale bars: A= 200um, applies to C, D, F, H, I, K, M, N, P, R, S; A′= 50um, applies to B, E, F′, G, J, K′, L, O, P′, Q, T.

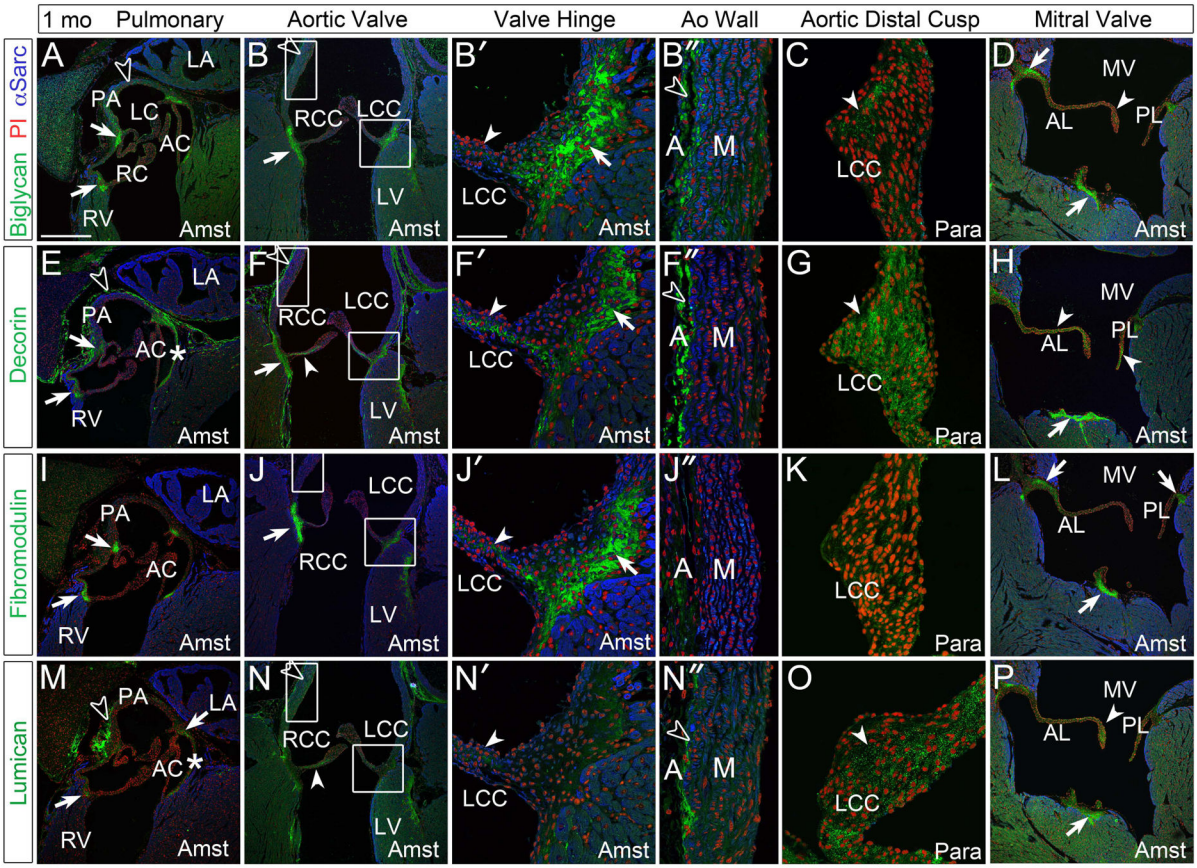

Figure 4. At 1 month, biglycan, decorin, fibromodulin, and lumican were immunolocalized within collagen rich structures including the cardiac valves and arterial walls of the maturing heart

A–D: Biglycan (green), **E–H:** decorin (green), **I–L:** fibromodulin (green) and **M–P:** lumican (green) immunolocalization. Boxes magnified in adjacent panels and designated with a prime. *-annulus region associated with the anterior cusp (AC) of the pulmonary valve (PV); solid arrows-regions where valve cusps or leaflets anchor into adjacent tissue; solid arrowheads- staining within the cusps or leaflets; open arrowheads- arterial wall staining; LC-left cusp of the PV; RC-right cusp of the PV; RV- right ventricle; PA-pulmonary artery wall; LA-left atrium; RCC- right coronary cusp of the aortic valve (AV); LCC- left coronary cusp of the AV; LV-left ventricle; A-adventitia of aorta; M-medial layer of aorta; MV-mitral valve; AL-anterior leaflet; PL-posterior leaflet; Para- paraformaldehyde fixed tissue; Amst- Amsterdam fixed tissue. Blue- alpha sarcomeric actin; red- propidium iodide. Scale bars: A= 200um, applies to B, D, E, F, H, I, J, L, M, N, P; B′= 50um, applies to B″, C, F′, F″, G, J′, J″, K, N′, N″, O.

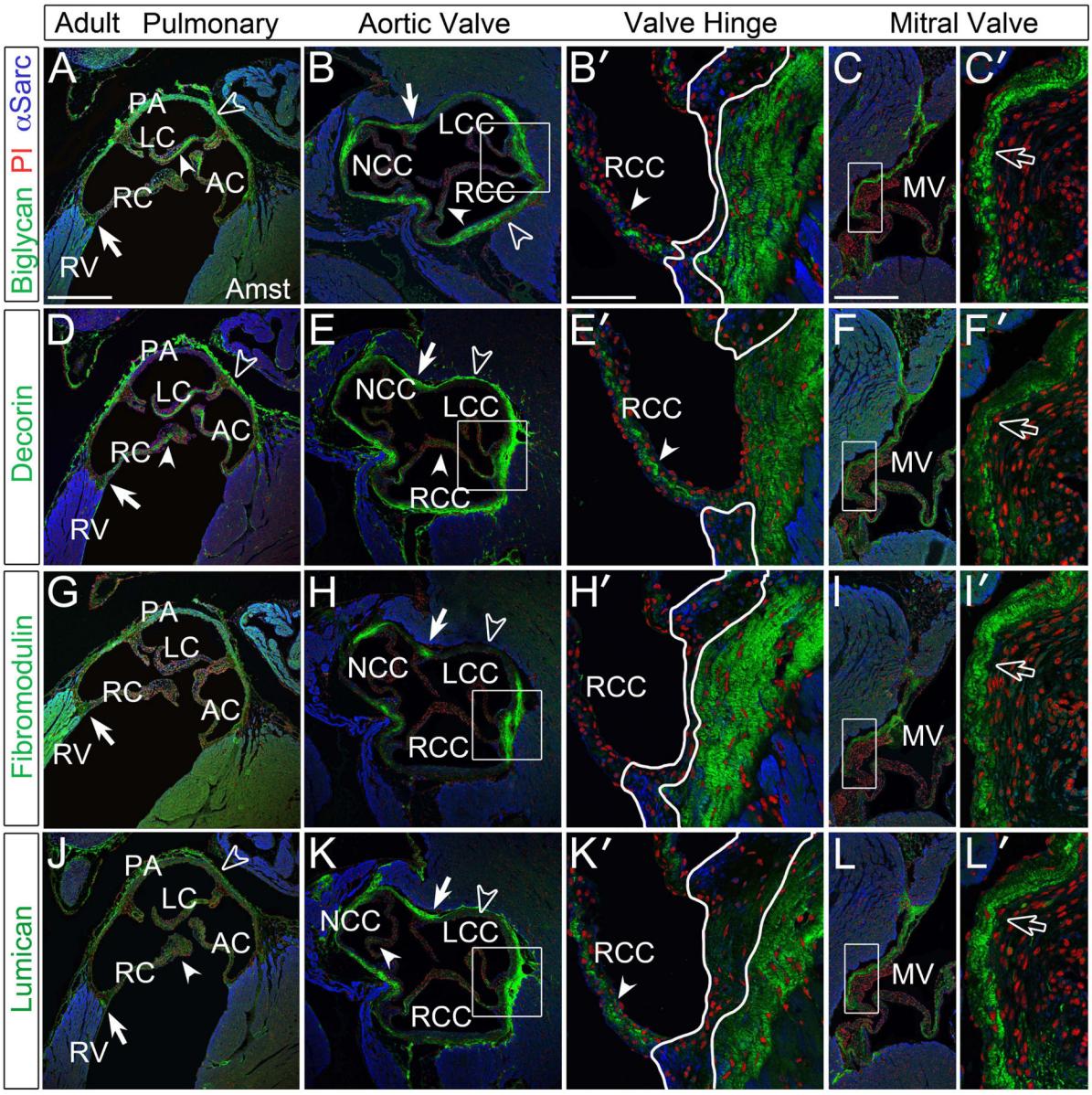

Figure 5. Immunolocalization of SLRPs in adult murine hearts demonstrated high levels of expression within the cardiac valves and arterial walls of the aortic and pulmonary arteries

A–C′: Biglycan (green), **D–F′:** decorin (green), **G–I′:** fibromodulin (green), **J–L′:** lumican (green) immunolocalization in the cardiac valves and arterial walls. Boxes in panels B, C, E, F, H, I, K, L magnified in adjacent panels designated with a prime. White outline in B′, E′, H′, and K′ show variability of regions void of SLRP staining. Arrowheads- staining within the cusps and leaflets; solid arrows- cusp/leaflets attachment sites; open arrowheads- staining in the arterial wall; open arrows- staining in the mitral valve leaflets. PV-pulmonary valve; AV-aortic valve; RV- right ventricle; RC-right cusp of the PV; LC- left cusp of the PV; AC-anterior cusp of the PV; NCC- non-coronary cusp of the AV; RCC- right coronary cusp of the AV; LCC- left coronary cusp of the AV; MV- mitral valve; Amst- amsterdam fixed tissue (applies to all panels). Blue- alpha sarcomeric actin; red- propidium iodide.

Scale bars: A= 400um, applies to B, D, E, G, H, J, K; B′= 50um, applies to C′, E′, F′, H′, I′, K′, L′; C= 200uL, applies to F, I, L.

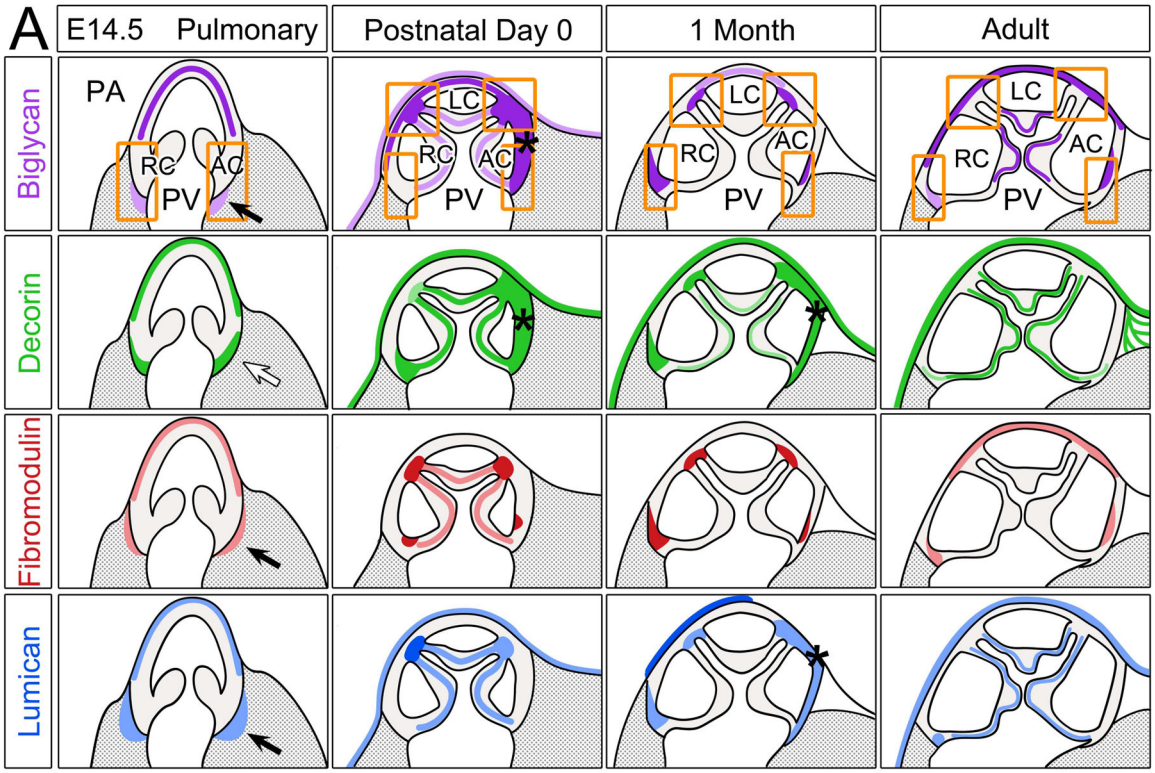

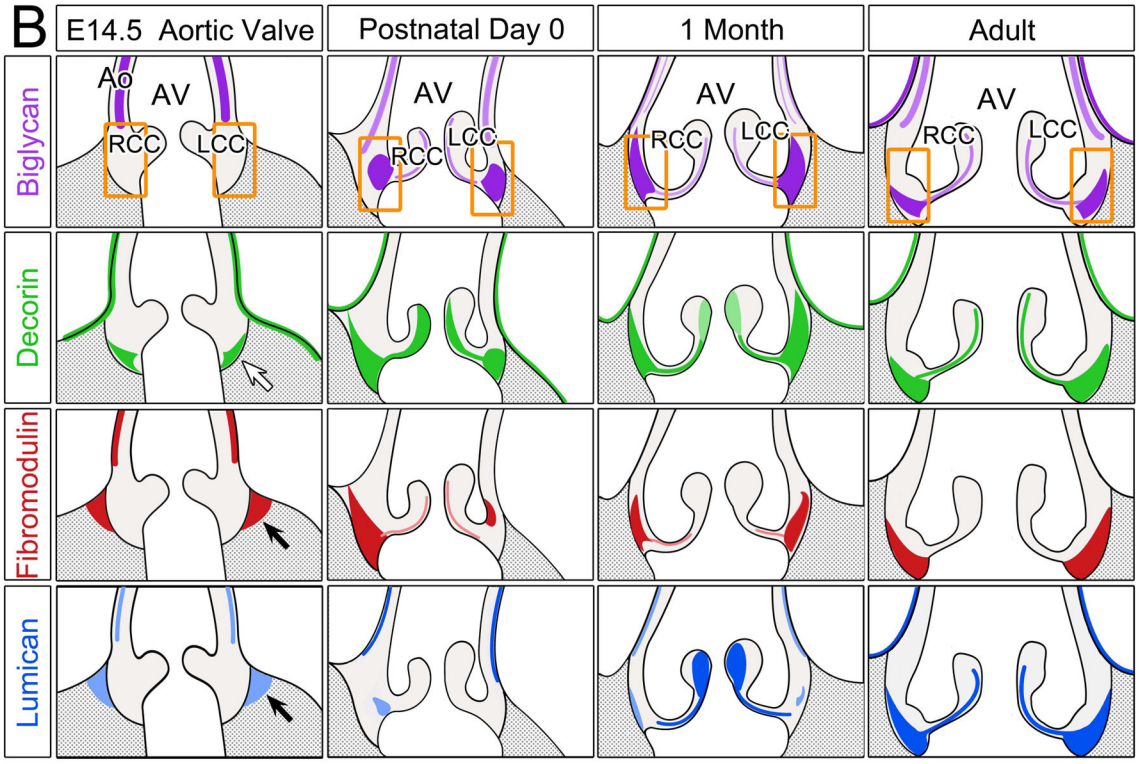

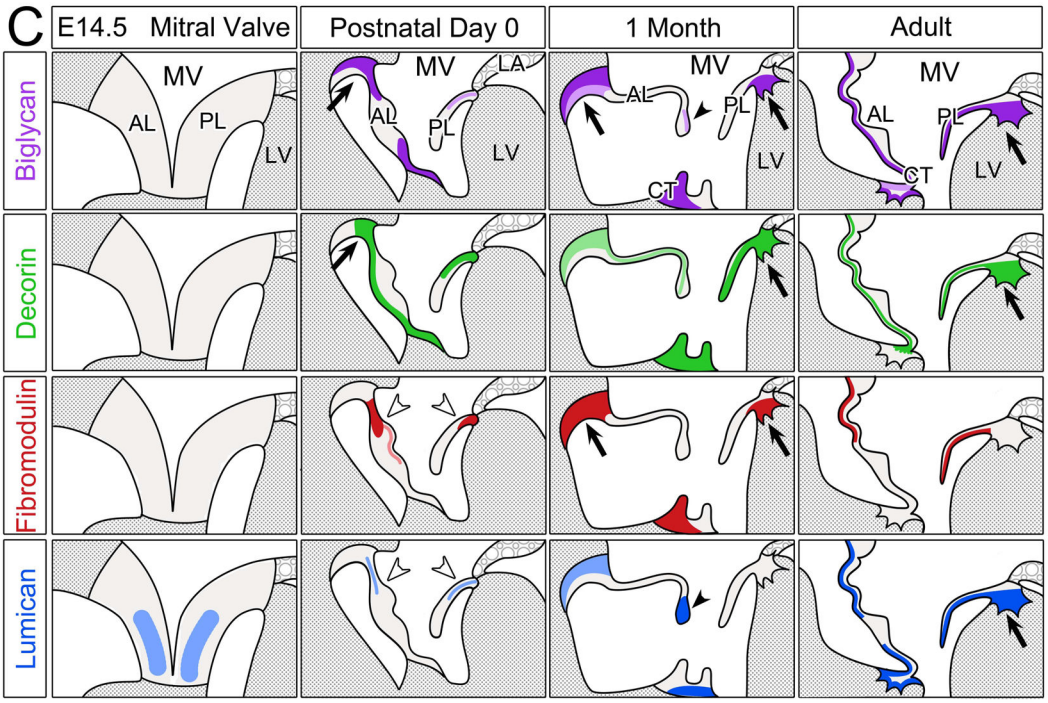

Figure 6. Schematic summary of biglycan, decorin, fibromodulin and lumican in the murine cardiac valves

Schematics depicting the expression profiles of class II SLRPs from E14.5 to adult in the **A** pulmonary valve and the arterial wall of the pulmonary artery**, B** aortic valve and aortic wall, and **C** the mitral valve. Images depict the summary of the IHC patterns for biglycan (BGN, purple), decorin (DCN, green), fibromodulin (FMOD, red) and lumican (LUM, blue). The general trends of IHC intensity are depicted by the shades of individual colors, i.e. dark shades equal high signal intensity and light shades indicate lighter signal intensity. Orange rectangles-regions where valve cusps anchor at the base of the ventricles; orange squares-regions where cusps anchor within the arterial walls; *-staining within the annulus associated with the AC cusp of the pulmonary valve (PV). PA-pulmonary artery; RC-right cusp of the PV; AC-anterior cusp of the PV; LC-left cusp of the PV; Ao-arterial wall of the aortic artery; AV- aortic valve; RCC-right coronary cusp of the AV; LCC-left coronary cusp of the AV; MV-mitral valve; AL-anterior leaflet of the MV; PL-posterior leaflet of the MV; LV-left ventricle; LA-left atrium; CT-chordae tendineae. Open arrow- localization in the prevalvular mesenchyme adjacent to the myocardium; solid arrow-staining within the myocardium adjacent to the valve mesenchyme; open arrowheads- staining within the base of the MV; solid arrowheads-staining within the tip of the MV; ▩-denotes ventricular myocardium; ▩-denotes atrial myocardium.